Northumbria Research Link

Northumbria
University
NEWCASTLE

Influence of light coupling configuration and alignment on the stability of HWG-based gas sensor system for real-time detection of exhaled carbon dioxide

Tao Zhou, Tao Wu*, Huailin Zhang, Qiang Wu**, Weidong Chen, Chenwen Ye, and Xingdao He

***Abstract*—A mid-infrared tunable diode laser absorption spectroscopy (TDLAS) gas sensor based on hollow waveguide (HWG) gas cell for real-time exhaled carbon dioxide (eCO_2) detection is reported. A 2.73 μm distributed feedback (DFB) laser was used to target a strong CO_2 absorption line, and wavelength modulation spectroscopy (WMS) with the second harmonic (WMS-2*f*) was used to retrieve the CO_2 concentration with high sensitivity. The influence of different parameters, including coupling configuration of HWG, laser-to-HWG and HWG-to-detector coupling alignment on the stability of the HWG sensor is systematically studied. The HWG eCO_2 sensor showed a fast response time of 2.7s, detection limit of 17 ppmv, and measurement precision of 20.9 ppmv with a 0.54 s temporal resolution. The eCO_2 concentrations changed in breath cycles were measured in real time. The Allan variance indicated that the detection limit can reach 1.7 ppmv, corresponding to a detection sensitivity of 1.3×10^{-8} $cm^{-1}Hz^{-1/2}$, as the integration time increases to 26 s. This work demonstrates the performance characteristics and merits of HWG eCO_2 sensor for exhaled breath analysis and potential detection for other exhaled gases.**

***Index Terms*—tunable diode laser absorption spectroscopy, hollow waveguide, distributed feedback laser, carbon dioxide**

I. Introduction

BREATH ANALYSIS can provide a non-destructive, real-time disease diagnosis and metabolic state monitoring, and hence plays a very important role in the field of medical diagnostics. Human breathing gases contain several kinds of gases, such as N_2, O_2, CO_2, H_2O with a relatively high concentrations accounting for more than 99% of the total content, and hundreds of other kinds of breathing gases, such as acetone, methane, ammonia, carbon monoxide etc. in the concentration levels varies from parts per million by volume (ppmv) to parts per trillion by volume (pptv) [1]. Some of these respiratory gases have been proven to be useful as biomarkers for metabolic monitoring and disease diagnosis [2]. The changes in exhaled CO_2 (eCO_2) concentration as well as the end-tidal CO_2 concentration is important for some early disease diagnosis and physiological monitoring of the human body [3], while eCO_2 analysis requires high sensitivity/stability, excellent selectivity and well-designed breath sampling systems.

Laser absorption spectroscopy has been widely used in gas detection and plays an important role in industrial process analysis, environmental pollution monitoring, scientific research and other fields [4]. Due to its medical interest, in recent years a variety of spectroscopy techniques have been developed to detect CO_2 and $^{13}CO_2/^{12}CO_2$ isotopic ratio in exhaled breath. Non-dispersive infrared spectroscopy (NDIR) is commonly used for the detection of eCO_2 [5]-[7]. NDIR measures the gas concentrations by detecting the infrared light attenuation using a photo detector. Commercial NDIR CO_2 capnographs work very well with high target gas selectivity and do not need frequent calibration, however, it usually possesses low sensitivity and faces interference from water vapor and hydrocarbons. Beyond that method, high finesse optical cavity based absorption spectroscopy, such as cavity ring-down spectroscopy (CRDS) [8] and integrated cavity output spectroscopy (ICOS) [9], and tunable diode laser absorption spectroscopy (TDLAS) with a multi-pass cell have also been widely used for eCO_2 detection [10], [11]. The use of high finesse optical cavity and multi-pass cell significantly increases the absorption path length and improves the detection sensitivity. However, these conventional systems have disadvantages of rigid requirement of precision optical light alignment, high cost, large physical size and especially large volume (usually larger than 100 ml) resulting in unsuitable for real time exhaled gas measurement [9], [12]. Hollow waveguide (HWG) possesses a low volume and an extended optical path length that gives absorption spectroscopy a fast response time and high sensitivity with lower cost [13], [14]. Several authors have reported the use of HWG gas cells in absorption spectroscopy using TDLAS or Fourier transform infrared spectroscopy (FTIR). Xiong et al. [15] designed an HWG based CO_2 sensor for capnography using direct absorption spectroscopy. Kim et al. [16]

This work is supported by the Key Research and Development Program of Jiangxi Province, China (20171BBG70003, 20192BBH80019), the Ministry of Human Resources and Social Security of China.

Tao Wu is with the Key Laboratory of Nondestructive Test (Ministry of Education) of Nanchang Hangkong University, Nanchang 330063, China. (e-mail: wutccnu@nchu.edu.cn).

Qiang Wu is with the Department of Physics and Electrical Engineering, Northumbria University, Newcastle upon Tyne, U.K. (e-mail: qiang.wu@northumbria.ac.uk).

established a gas sensor with an HWG combined with an FTIR spectrometer for CO_2 and CH_4 detection.

All present studies are mainly focused on the improving coupling efficiency of laser to HWG [17], [18]. However stability is a significant parameter for an HWG-based sensor system, which is mainly limited by temperature drifts, mechanical vibrations, and moving fringes in background spectra, and usually described by the Allan variance. However, the investigation of the effect of laser-to-HWG and HWG-to-detector coupling alignment on stability of HWG-based sensor system is missing in the previous literatures. In this paper, a mid-infrared HWG eCO_2 sensor employing a 1 m long HWG was developed for real-time eCO_2 detection. Second harmonic (WMS-2f) wavelength modulation spectroscopy (WMS) was applied for eCO_2 detection. A systematic study of the influence of sensor system parameters, including coupling configuration of HWG, laser-to-HWG and HWG-to-detector coupling alignment on the stability of the HWG sensor was performed. Our study shows that, Laser-to-HWG and HWG-to-detector coupling alignment play more important role to the stability of the sensor system, which provides a new guide for improving stability of the system. Finally, real time experiment for eCO_2 was conducted to evaluate the performance of HWG eCO_2 sensor for medical requirement.

II. WMS METHOD

The application of WMS in TDLAS can effectively improve the detection sensitivity and has been widely used in the measurement of absorption spectroscopy [19]. In WMS-2f method, the injection current of the DFB laser is modulated by the sawtooth wave superimposed with a high-frequency sinusoidal signal. The frequency (wavelength) $\nu(t)$ and intensity $I_0(t)$ of the laser are also modulated accordingly [20].

$$\nu(t) = \bar{\nu} + a\cos(2\pi ft) \tag{1}$$

$$I_0(t) = \overline{I_0}\left[1 + i_0\cos(2\pi ft + \psi_1) + i_2\cos(2\cdot 2\pi ft + \psi_2)\right] \tag{2}$$

Where $\bar{\nu}$ is the average laser frequency (wavelength); a and f are the amplitude of wavelength modulation and modulation frequency, respectively; $\overline{I_0}$ is the average laser intensity; i_0 and i_2 are the Fourier coefficients of the linear and non-linear intensity modulations; ψ_1 and ψ_2 are the phase shift of the linear and non-linear intensity modulations, respectively. For weak absorption ($\alpha(\nu) < 0.05$), the absorption can be expanded into the Fourier cosine.

$$\alpha[\bar{\nu} + a\cos(2\pi ft)] = -\sum_{k=0}^{\infty} H_k(\bar{\nu}, a)\cos(k\cdot 2\pi ft) \tag{3}$$

Here, H_k is the k_{th} harmonic component of the absorbance α .

$$H_k(\bar{\nu}, a) = -\frac{1}{2\pi}\int_{-\pi}^{\pi}\alpha(\bar{\nu} + a\cos\theta)\,d\theta, k = 0 \tag{4}$$

$$H_k(\bar{\nu}, a) = -\frac{1}{\pi}\int_{-\pi}^{\pi}\alpha(\bar{\nu} + a\cos\theta)\cos k\theta d\theta, k \geq 1 \tag{5}$$

For the WMS-2f detection, a reference signal with a frequency of 2f is sent to the lock-in amplifier, and the X-channel of the modulation signal (the in-phase signal) can be expressed as follows.

$$X_{2f} = \frac{G\overline{I_0}}{2}\left[H_2 + \frac{i_0}{2}(H_1 + H_3)\cos\psi_1 + i_2\left(1 + H_0 + \frac{H_4}{2}\cos\psi_2\right)\right] \tag{6}$$

Here G account for the optical-electrical gain of the detection system. Usually, i_2 is much smaller than i_0. For an isolated transition, the odd term of the Fourier coefficient at the center of the spectrum line is zero. The relationship between the peak value $X_{2f}(\bar{\nu})$ of the WMS-2f signal and the mole fraction x of the target gas can be calculated as.

$$X_{2f}(\bar{\nu}) \approx \frac{G\overline{I_0}}{2}H_2(\bar{\nu}) = -\frac{G\overline{I_0}PSxL}{2\pi}\int_{-\pi}^{\pi}\phi(\bar{\nu} + a\cos\theta)\cdot\cos 2\theta\cdot d\theta \tag{7}$$

Where P and L are the total gas pressure and the effective optical path length, respectively. S and ϕ are the line strength and line shape function, respectively.

III. LINE SELECTION

According to the HITRAN database [21], CO_2 has strong absorption lines in the mid-infrared region. For the eCO_2 detection, the main interfering gas is H_2O. Apart from H_2O, the concentrations of other potential interference in breathing gases are 10^4-10^{10} times smaller than that of eCO_2, which make their influence negligible. To eliminate the interference from H_2O, the CO_2 absorption line was selected at 3661.637 cm^{-1} with a line strength of 7.135×10^{-22} cm^{-1}/(molecule·cm^{-2}), which has no overlap with that of H_2O. Fig. 1 shows the simulation of the absorption spectrum of 5% H_2O and 5% CO_2 for wavenumber range from 3657.57 cm^{-1} to 3665.95 cm^{-1} at a pressure of 270 torr and a temperature of 296 K. The inset of Fig. 1 shows the selected absorption line at 3661.637 cm^{-1}. It is worth noting that the choice of absorption line also considers the characteristics of the laser. The stronger absorption line at 3663.851cm^{-1} has not been selected, because it is out of the wavelength tuning range of the laser used in our experiments.

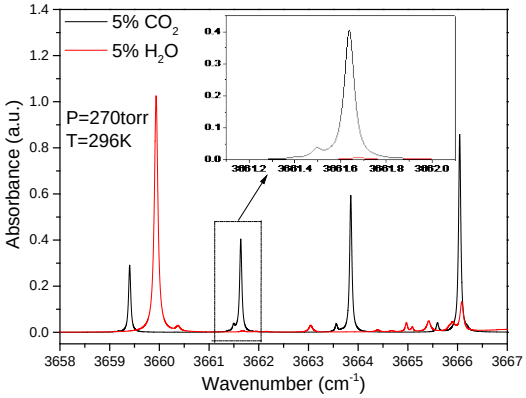

Fig. 1. The simulation of the absorption spectrum of 5% H_2O and 5% CO_2 at 270 torr and 296 K. The inset shows the selected absorption line at 3661.637 cm^{-1}.

IV. Experiment Setup

The eCO_2 sensor based on HWG is shown in Fig. 2(a). A DFB laser (Nanoplus GmbH, Germany) with a center wavelength of 2.73 μm and a maximum output power of 11.2 mW was used as an optical source. The laser was packaged in a TO-5 can with integrated Peltier and temperature sensor, which attached to an aluminum heatsink to remove heat dissipated from Peltier and the laser. A laser controller (ILX Lightwave, LDC-3724C, USA) was used to control the current and temperature of the laser diode. The current of the laser was set to 148.39 mA, and the operating temperature of the laser was set and controlled at 30 ºC. High-frequency sine wave (1.7 kHz) generated by a lock-in amplifier (Stanford Research System, SR830, USA) and a sawtooth wave (20 Hz) generated by a function generator were superimposed by an adder, and then sent to the modulation current port of the laser controller for performing WMS. The laser beam was collimated by a collimating lens and coupled through an aperture diaphragm into a 1 m long and 1 mm inner diameter HWG (Polymicro Technologies, HWEA10001600, USA) gas cell with the volume of 0.78 cm^3, which was much smaller than that of the conventional multi-pass gas cell. The HWG fiber was firstly inserted into a fiber ferrule, and then inserted into the slot in the gas chamber and sealed with a layer of silicone rubber outside the chamber as shown in Fig. 2(b). The light output from the HWG cell was detected by a photodetector (VIGO System S.A., PVI-4TE-10.6, USA). The lock-in amplifier demodulated the output signal of the photodetector to obtain the WMS-2f signals, which was then acquired by a data acquisition card (ADlink, DAQ-2010, China) and further processed by a self-developed LabWindows program. The modulation parameters, such as modulation amplitude, modulation frequency, reference phase, time constant of lock-in amplifier, and laser scanning frequency, and gas pressure in the HWG were optimized by obtaining maximum detection WMS-2f signal. In order to reduce the CO_2 interference from the air, the laser and the photodetector were placed very close to the HWG cell. For exhaled CO_2 measurement, most breathing gas exhaled through a mouthpiece was vented to the atmosphere through the small gap between breath sampler and breath tube, while a part of the sample was continuously drawn to the HWG cell through breath tube by a vacuum pump (DIVAC, 1.2 L, Germany). A mass flow controller (MFC, MKS Instruments, USA) and a pressure controller (MKS Instruments, 640B, USA) were used to control constant gas flow rate and stable pressure in the HWG cell.

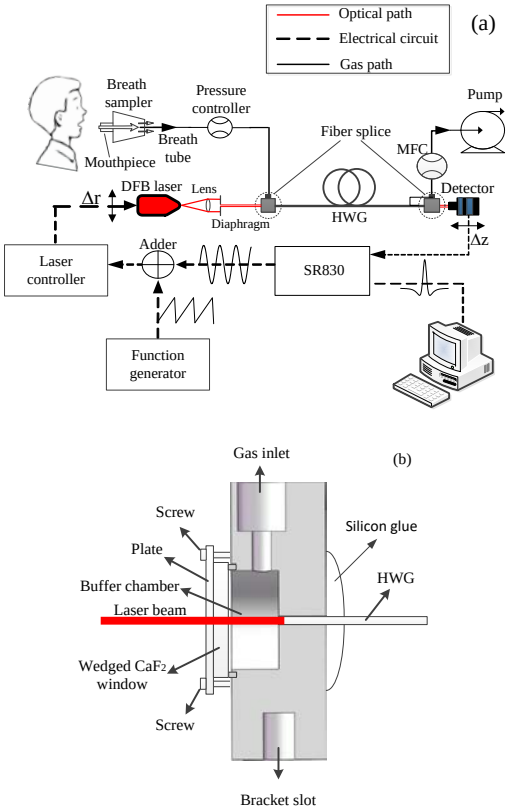

Fig. 2. Schematic of the experimental setup (a) and the optical fiber splice (b).

V. The Coupling Pattern of Laser Beam to HWG and Its Effect on System SNR and Stability

The coupling configuration between the laser beam and the HWG can be achieved in a focusing coupling configuration or in a direct coupling configuration (incident directly into the HWG). Here, the focusing coupling configuration and the direct coupling configuration are both studied. The influence of the laser spot size (modulated by an aperture diaphragm) on direct coupling configuration is considered. The stability of the system for these two coupling mode is explored. The relation between stability time and SNR of direct coupling configuration is investigated.

5% CO_2 was continuously pumped into the HWG cell, and the pressure in the cell was controlled at 270 torr. In the focusing coupling configuration, the laser beam is focused into the center of the HWG inlet by a lens with a focal length of 50mm. In the direct coupling configuration, the aperture size of the aperture diaphragm was sequentially set to 0.7 mm, 1 mm, 1.5 mm, 2 mm, 2.3 mm, where 0.7 mm is the minimum aperture that can be set by the aperture diaphragm used in our experiment, and 2.3 mm is the actual size of the laser beam.

The WMS-2f signals for focusing coupling and direct coupling with different spot sizes were recorded and shown in Fig. 3. It can be seen that the SNR for focusing coupling is highest. For direct coupling configuration, as the spot size decreases, the SNR decreases, this is due to a gradual reduction of the laser power. Fig. 4 shows the Allan variance obtained by measuring WMS-2f signals. It can be clearly seen that, although the focusing coupling has highest SNR, the system stability for focusing coupling is worse (with higher variance limit) than that of direct coupling with 1 mm spot. As the spot diameter decreases from 2.3mm to 0.7mm, the system stability time for direct coupling is increased from 6 s to 57 s, which is possibly due to the fact that smaller aperture and acceptance angle collects center of the laser beam which has better laser beam quality illuminated to the HWG, resulting in small fiber model noise. However, the smaller aperture results in smaller SNR (as shown in Fig. 5), which is not conducive to improving the detection sensitivity (As the aperture is gradually reduced, the detection sensitivity is reduced from 7.9×10^{-6} $cm^{-1}Hz^{-1/2}$ to 1.8×10^{-6} $cm^{-1}Hz^{-1/2}$). Here, direct coupling with the aperture of 1 mm reaches a compromise between good SNR and long stability time.

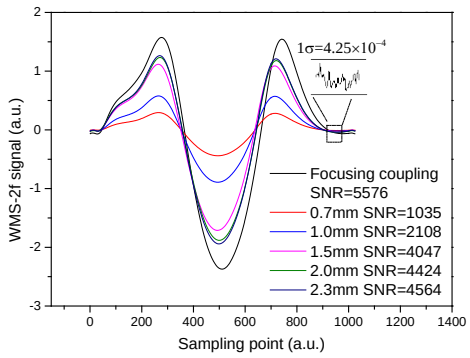

Fig. 3. The WMS-2f signals for focusing coupling and direct coupling with different spot sizes.

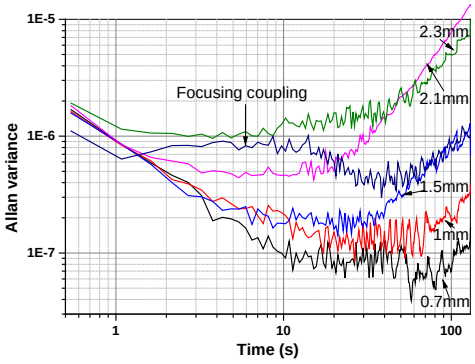

Fig. 4. The Allan variance obtained by measured WMS-2f signals.

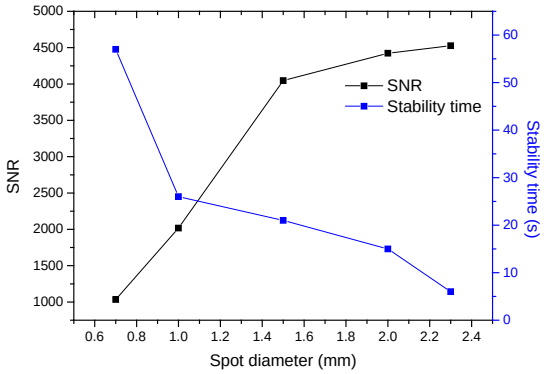

Fig. 5. The relation between stability time and SNR of the system as the spot diameter changes.

For direct outcoupling, possible parallel optical surfaces interference caused by focusing lens is avoided. To study the effect of partial collection of light from the fiber on system stability, the distance between the output of HWG and the detector was varied between -200μm and 200μm based on initial distance of 4cm. An optimal detector displacement distance Δz was found at -40μm (Fig. 6). It is noted that this optimal value obtained in the experiments is for our setup only. The detector is suggested to be placed as close as possible to the fiber end to collect all the light coming from the fiber end for any HWG-based setup. The influence of incoupling (position of the laser) on system stability was also investigated. The lateral displacement Δr between the center of laser beam and the center axis of HWG was varied from 0 to 120μm in 40μm steps. We found the laser at the central position given longest stability time (Fig. 7).

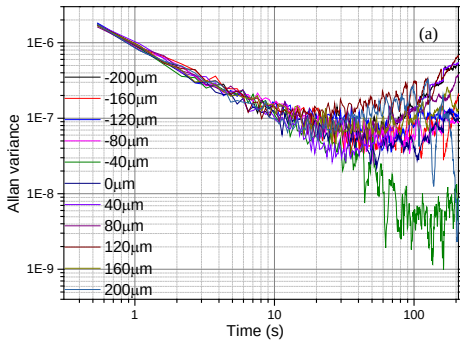

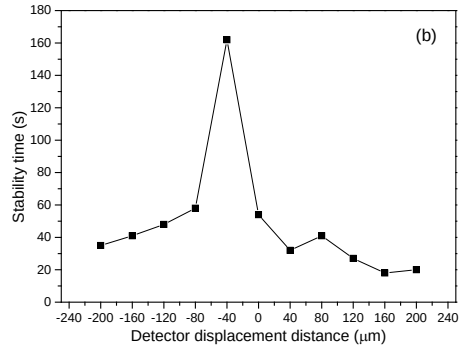

Fig. 6. (a) The Allan variance for WMS-2f signals at varied displacement distance of detector; (b) Stability time versus detector displacement distance.

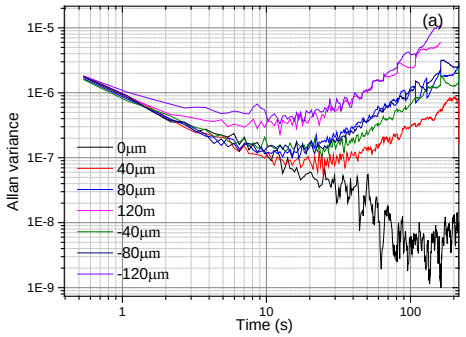

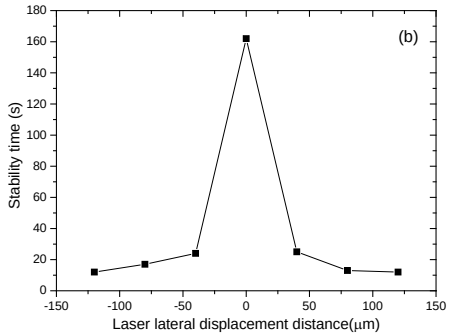

Fig. 7. (a) The Allan variance for WMS-2f signals at varied displacement distance of laser; (b) Stability time versus laser lateral displacement distance.

VI. Investigation of Response Time and Concentration Calibration

The response time of the HWG eCO_2 sensor was investigated as shown in Fig. 8. Two mass flow controllers controlled the flow rate of pure CO_2 gas ($CO_2 \geq 99.999\%$) and pure nitrogen gas ($N_2 \geq 99.999\%$) respectively. Five different samples of CO_2 with concentrations varying from 0 to 6.3% were prepared by changing the flow rates of two mass flow controllers while maintaining a constant gas flow rate of 6.7 ml/s through the HWG cell. The pressure in the HWG cell was controlled to be 270 torr for obtaining WMS-2f signal. In the beginning, the HWG cell was full of pure nitrogen. Then, at 40 s, the diluted CO_2 gas samples were filled into the HWG cell. The duration time of each concentration level gas sample was approximately 30 s to ensure that the measured signal was in a stable state. At the end of the measurement, pure nitrogen was again filled into the HWG cell. There was no significant drift found during the measurement period by the nitrogen signal levels. As shown in the insert of Fig. 8, the response time τ_r (10 - 90%) of the concentration levels in rising and falling process was about 2.7 s and 2.2 s, respectively, while the delay time τ_d (0 - 10%) was approximately in the same time of 0.6 s [22]. Due to the smaller volume of the HWG than the traditional gas cell ($\tau_r \sim 5$ min) [12], the response time τ_r is much faster compared to the traditional gas cell with the similar gas flow rate. It is worth noting that the response time τ_r here also included the time for gas mixing time in the HWG cell, the actual response time of the HWG sensor was less than 2.7 s.

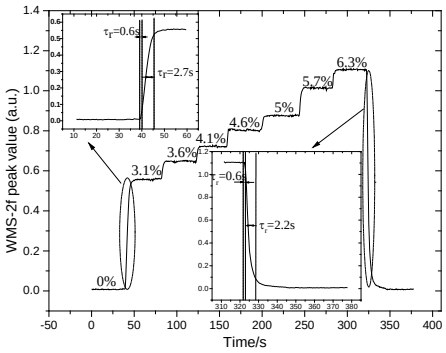

Fig. 8. Continuous measurements for different CO2 concentration levels.

In order to obtain the relationship between WMS-2f peak values and CO_2 concentrations, CO_2 samples were prepared by using pure CO_2 gas and 3000 ppmv standard CO_2 gas diluted with pure N_2, and the continuous measurements for different CO_2 concentration samples were performed and averaged 5 times with a 100 ms acquisition time. Fig. 9(a) shows the WMS-2f signals at different CO_2 concentrations with a 0.5 s temporal resolution. A linear relationship between WMS-2f peak values and CO_2 concentrations was observed as shown in Fig. 9(b). Fig. 9(b) shows the fit curve have a good linearity for CO_2 concentrations varied from 0-6.3%, even down to 200ppmv, which were used as calibration model to determine CO_2 concentrations. The error bars of the WMS-2f peak values were in the order of 10^{-3}, which cannot be clearly seen in Fig. 9(b).

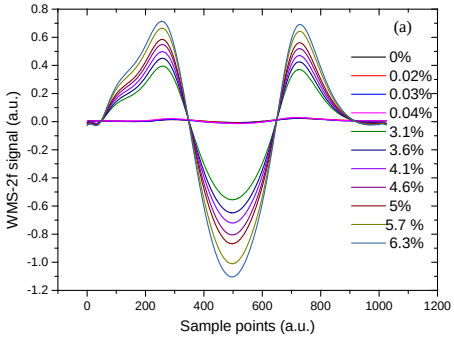

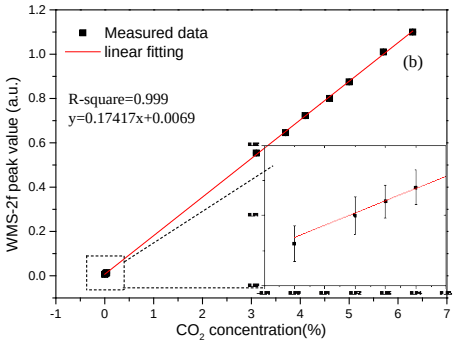

Fig. 9. The calibration results of CO_2 concentrations. (a) The WMS-2f signals at different CO_2 concentrations; (b) Relationship between measured WMS-2f peak values and different CO_2 concentrations.

VII. Measurement Precision

The measurement precision of the HWG eCO_2 sensor can be analyzed by Gaussian distribution [23]. 300ppmv diluted CO_2 gas sample was used as reference gas and pumped into the HWG cell. The gas pressure and flow rate were maintained at 270 torr and 6.7 ml/s, respectively. 600 measured data points were successively recorded and averaged 5 times corresponding to 0.54 s temporal resolution, as shown in Fig. 10(a). A histogram plot of CO_2 concentration deviation which is fitted by a Gaussian profile is shown in Fig. 10(b). The measurement precision can be determined by the half width at half maximum (HWHM) of the Gaussian profile. It indicates that the measurement precision was 20.9 ppmv with 0.54 s temporal resolution. The corresponding average concentration value was 297 ± 20.9ppmv. The measurement precision was mainly limited by random noise and etalon fringes superimposed on the WMS-2f signals. In addition, the small jitter of the HWG would lead to instability of the WMS-2f signals, which also affected the measurement precision.

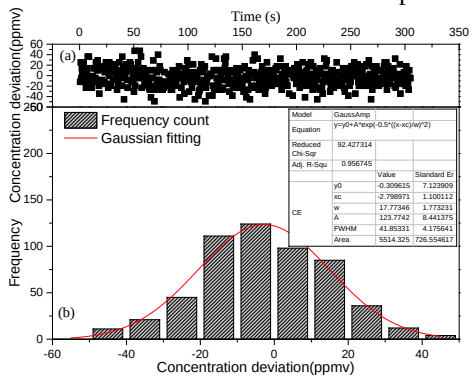

Fig. 10. (a) 600 measured data points were successively recorded and averaged 5 times corresponding 0.54 s temporal resolution; (b) A histogram plot of CO_2 concentration deviation which is fitted by a Gaussian profile.

VIII. Carbon Dioxide in Exhaled Breath

The eCO_2 was measured in real time from one healthy volunteer in our lab and the results recorded with 0.54 s acquisition time are shown in Fig. 11. The pressure in the HWG cell was controlled to be 270 torr, and the breathing gas was introduced into the HWG cell by breath tube according to the direction of gas passage shown in Fig. 2. During the inhalation, the environment air was pumped into HWG through the side-port of breath tube, and the CO_2 concentrations are stable and fluctuated around 360ppmv as shown in Fig. 11, hence the influence of ambient air on eCO2 detection can be negligible. In addition, the trends and values of concentration which are not affected by the breath rate changes were consistent with those in the literatures [24], [25]. It is noted that the response time τ_r of 3.7 s in this case is larger than that of 2.7 s described above. This is possibly due to the contribution of residual eCO_2 in long breath tube during exhalation. If the volume of breath tube is made smaller and the length of breath tube is shorter, the response time will be faster.

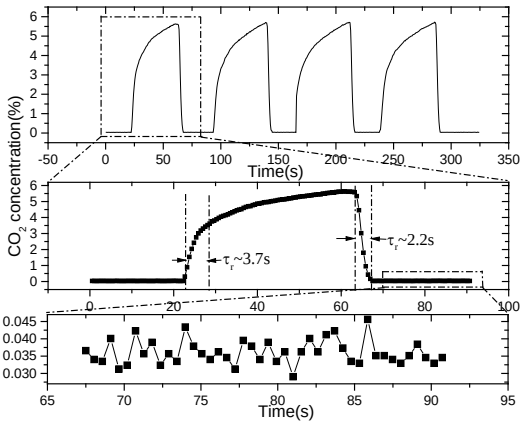

Fig. 11. Concentration dynamics of eCO2 in real time from one volunteer in our lab.

IX. Detection Limit

The signal averaging method is a simple but practical method for eliminating background white noise. If a signal is averaged N times, the white noise may be reduced by a factor of $N^{1/2}$, which can be estimated by Allan variance [26]. Allan variance can evaluate the stability of the measurement system as well as the detection limit. Allan deviation was performed on a constant concentration of 300ppmv diluted CO_2 sample which was pumped into HWG cell continuously, and Allan deviation (square root of variance) plot was shown in Fig. 12. The results shows that the Allan deviation decreases with the square root of the averaging time (shown in Fig. 12 as the red line of gradient = −0.5). The detection sensitivity was 17 ppmv with acquisition time of 0.54 s, corresponding to a detection sensitivity of 6.9×10^{-8} $cm^{-1}Hz^{-1/2}$, which indicates that the TDLAS sensor is applicable for clinical eCO_2 monitoring. The minimum in the Allan deviation plot at 26 s represents the optimum integration time. The detection limit can reach as low as 1.7 ppmv, corresponding to a detection sensitivity of 1.3×10^{-8} $cm^{-1}Hz^{-1/2}$, as the integration time increases to 26 s. Thereafter the Allan deviation moves into a drift dominated region where it starts to increase with increasing averaging time. Furthermore, the detection limit can be further improved by increasing HWG length, reducing hardware noise and fixing the HWG firmly to suppress the etalon signal. Table 1 shows the detection limit and other experimental parameters

obtained by using different methods to measure eCO_2. Though direct absorption spectroscopy (DAS) used in ref. [10], [11], [15] is calibration-free, the DAS is mainly limited by $1/f$ noise. The WMS uses a higher modulation frequency (~kHz) which suppresses the $1/f$ noise effectively, which is verified in Table I that the absorbance sensitivity (independent of optical length and related to stability of system) for WMA is usually higher than that for DAS. It is noted that the absorption sensitivity of the HWG sensor can be improved significantly by adding two high reflectivity mirrors to both ends of the HWG to form a high finesse resonant cavity, which effectively increases the length of optical path [8].

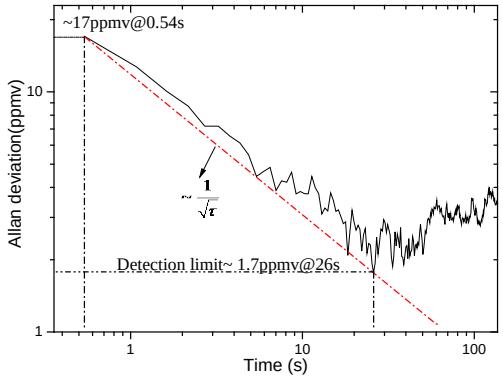

Fig. 12. Allan deviation plot for measured 300ppmv CO_2 sample.

TABLE I
DETECTION LIMIT AND OTHER EXPERIMENTAL PARAMETERS FOR ECO_2 DETECTION USING DIFFERENT METHODS

Reference	Wavelength (μm)	Pressure (torr)	Optical length (m)	Method	Detection limit/Absorbance sensitivity
[10]	4.91	380	26	TDLAS/ DAS (Multipass cell)	0.5%/~10^{-2}
[11]	2	760	0.025	TDLAS/ DAS (Single cell)	<300 ppmv/~10^{-4}
[15]	2.003	760	0.12	TDLAS/ DAS (HWG cell)	10 ppmv/~10^{-5}
[27]	1.575	150	40	TDLAS/ WMS (Multipass cell)	100 ppmv/~10^{-4}
[28]	4.7	100	4	WMS (Multipass cell)	2ppmv/~10^{-6}
[7]	4.3	760	0.08	NDIR (Custom cell)	10 ppmv/-
[8]	1.6	100	0.42	CRDS	3 ppmv/~10^{-4}
Our present work	2.73	270	1	TDLAS/ WMS (HWG cell)	1.7 ppmv/~10^{-6}

X. CONCLUSIONS

A mid-infrared TDLAS gas sensor based on HWG gas cell for real-time eCO_2 detection is reported. An HWG with a length of 1 m was used as a gas chamber. Compared to SNR, laser-to-HWG and HWG-to-detector coupling alignment of light and HWG plays more important role to the stability of the sensor system. Due to the smaller volume (0.78 cm^3) of HWG, the response time of 2.7 s and 2.2 s in the rising and falling process was achieved. In addition, a detection limit of 1.7 ppmv corresponding detection sensitivity of 1.3×10^{-8} $cm^{-1}Hz^{-1/2}$ was reached at the optimal integration time of 26 s. It is shown that WMS can greatly improve the detection sensitivity and have a high measurement precision for CO_2 detection. HWG has a fast concentration response time and space saving features, and it is easy to develop into a compact portable instrument, which has practical significance for clinical respiratory detection. Furthermore, TDLAS has better selectivity to target the gas absorption line and has the potential for other exhaled gases detection.

REFERENCES

[1] J. Wojtas, Z. Bielecki, T. Stacewicz, J. Mikołajczyk, and M. Nowakowski, "Ultrasensitive laser spectroscopy for breath analysis," *Opto-Electron. Rev*., vol. 20, no. 1, pp. 26-39, Mar. 2012.

[2] C. Wang, and P. Sahay. "Breath analysis using laser spectroscopic techniques: breath biomarkers, spectral fingerprints, and detection limits," *Sensors*, vol. 9, no. 10, pp. 8230-8262, Oct. 2009.

[3] B. Braden *et al*., "^{13}C-breath tests: current state of the art and future directions," *Digest Liver Dis*., vol. 39, no. 9, pp. 795-805, Sep. 2007.

[4] R. W. Solarz, "Applications of Laser Absorption spectroscopy," in *Laser spectroscopy and its applications*, 10th ed., vol. 11, New York: Routledge, 2017, pp. 261-335.

[5] J. A. Vogt *et al*, "Optimised NDIR Technology for $^{13}CO_2$ Breath Tests of ie Drug/Drug-Interactions or Gastric Emptying for Intensive Care Patients: New Diagnostic Opportunities," in *WC*, Munich, Germany, Sep. 2009, pp. 851-854.

[6] K. Namjou, C. B. Roller, T. E. Reich, J. D. Jeffers, G. L. McMillen, P. J. McCann, and M. A. Camp, "Determination of exhaled nitric oxide distributions in a diverse sample population using tunable diode laser absorption spectroscopy," *Appl. Phys. B*., vol. 85, no. 2-3, pp. 427-435, Nov. 2006.

[7] T. A. Vincent, B. Urasinska-Wojcik and J. W. Gardner, "Development of a low-cost NDIR system for ppm detection of carbon dioxide in exhaled breath analysis," *Proc. Eng*., vol. 120, pp. 388-391, Sep. 2015.

[8] E. R. Crosson *et al*, "Stable isotope ratios using cavity ring-down spectroscopy: determination of $^{13}C/^{12}C$ for carbon dioxide in human breath," *Anal. Chem*., vol. 74, no. 9, pp. 2003-2007, Mar. 2002.

[9] M. R. McCurdy, Y. A. Bakhirkin, G. Wysocki, and F. K. Tittel, "Performance of an exhaled nitric oxide and carbon dioxide sensor using quantum cascade laser-based integrated cavity output spectroscopy," *J. Biomed. Opt.*, vol. 12, no. 3, pp. 034034, May. 2007.

[10] K. L. Moskalenko, A. I. Nadezhdinskii, and I. A. Adamovskaya, "Human breath trace gas content study by tunable diode laser spectroscopy technique," *Infrared Phys. Technol*., vol. 37, no. 1, pp. 181-192, Dec. 1996.

[11] A. Hartmann, R. Strzoda, R. Schrobenhauser, and R. Weigel, "CO_2 sensor for mainstream capnography based on TDLAS," *Appl. Phys. B.*, vol. 116, no. 4, pp. 1023-1026, Sep. 2014.

[12] K. Krzempek *et al*, "Continuous wave, distributed feedback diode laser based sensor for trace-gas detection of ethane," *Appl. Phys. B.*, vol.106, no. 2, pp. 251-255, Feb. 2012.

[13] J. A. Harrington, "A review of IR transmitting, hollow waveguides," *Fiber Integrated Opt*., vol. 19, no. 3, pp. 211-227, Oct. 2000.

[14] J. Chen, A. Hangauer, R. Strzoda, M. Fleischer, and M. C. Amann, "Low-level and ultralow-volume hollow waveguide based carbon monoxide sensor," *Opt. Lett.*, vol. 35, no. 21, pp. 3577-3579, Aug. 2010.

[15] B. Xiong, Z. Du, L. Liu, Z. Zhang, J. Li, and Q. Cai, "Hollow-waveguide-based carbon dioxide sensor for capnography," *Chin. Opt. Lett.*, vol. 13, no. 11, pp. 111201, Sep. 2015.
[16] S. S. Kim, N. Menegazzo, C. Young, J. Chan, C. Carter, and B. Mizaikoff, "Mid-infrared trace gas analysis with single-pass Fourier transform infrared hollow waveguide gas sensors," *Appl. Spectrosc*., vol. 63, no. 3, pp. 331-337, Apr. 2009.
[17] P. Patimisco *et al*, "Low-Loss Coupling of Quantum Cascade Lasers into Hollow-Core Waveguides with Single-Mode Output in the 3.7–7.6 µm Spectral Range," *Sensors* , vol. 16, no. 4, pp. 533, Apr. 2016.
[18] M. S. Vitiello *et al*, "High efficiency coupling of Terahertz micro-ring quantum cascade lasers to the low-loss optical modes of hollow metallic waveguides," *Opt. Express*., vol. 19, no. 2, pp. 1122-1130, Jan. 2011.
[19] J. Reid, and D. Labrie, "Second-harmonic detection with tunable diode lasers-comparison of experiment and theory," *Appl. Phys. B*., vol. 26, no. 3, pp. 203-210, Nov. 1981.
[20] H. Li, G. B. Rieker, X. Liu, J. B. Jeffries, and R. K. Hanson, "Extension of wavelength-modulation spectroscopy to large modulation depth for diode laser absorption measurements in high-pressure gases," *Appl. Optics*., vol. 45, no. 5, pp. 1052-1061, 2006.
[21] I. E. Gordon, *et al*, "The HITRAN2016 molecular spectroscopic database," *J. Quant Spectrosc. Ra*., vol. 203, pp. 3-69. Dec. 2017.
[22] J. Li, G. Luo, Z. Du, and Y. Ma, "Hollow waveguide enhanced dimethyl sulfide sensor based on a 3.3 µm interband cascade laser," *Sensor. Actuat. B-Chem*., vol. 255, pp. 3550-3557. Feb. 2018.
[23] J. Li, H. Deng, J. Sun, B. Yu, and H. Fischer, "Simultaneous atmospheric CO, N_2O and H_2O detection using a single quantum cascade laser sensor based on dual-spectroscopy techniques," *Sensor. Actuat. B-Chem*., vol. 231, pp. 723-732. Aug. 2016.
[24] R. Ghorbani, and F. M. Schmidt, "ICL-based TDLAS sensor for real-time breath gas analysis of carbon monoxide isotopes," *Opt. Express*., vol. 25, no. 11, pp. 12743-12752, May. 2017.
[25] D. Halmer, S. Thelen, P. Hering, and M. Mürtz, "Online monitoring of ethane traces in exhaled breath with a difference frequency generation spectrometer," *Appl. Phys. B*., vol. 85,no. 2-3, pp. 437-443. Nov. 2006.
[26] P. O. Werle, R. Mücke, and F. Slemr, "The limits of signal averaging in atmospheric trace-gas monitoring by tunable diode-laser absorption spectroscopy (TDLAS)," *Appl. Phys. B*., vol. 57, no. 2, pp. 131-139, Aug. 1993.
[27] V. Weldon, J. O'Gorman, P. Phelan, J. Hegarty, and T. Tanbun-Ek, "H_2S and CO_2 gas sensing using DFB laser diodes emitting at 1.57 µm," *Sensor. Actuat. B-Chem*., vol. 29, no. 1-3, pp. 101-107, Oct. 1995.
[28] R. Ghorbani, F. M. Schmidt, "Real-time breath gas analysis of CO and CO2 using an EC-QCL", *Appl. Phys. B.*, vol. 123, pp. 144, May 2017.

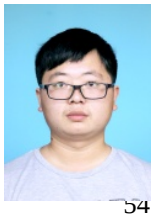

Tao Zhou received B.E. degree in photoelectric information science and engineering from School of Mechanical and Photoelectric Information Physics, Huaihua University in 2017. Since 2017, he has been a Graduate Student with the School of Measuring and Optical Engineering, Nanchang Hangkong University. His research interests include optical system design and gas absorption spectrum.

Tao Wu received his PH.D. degree in Optics from University of the Littoral Opal Coast and Anhui Institute of Optics and Fine Mechanics, China. In 2010, Dr. Wu joined Key Laboratory of Nondestructive Test (Ministry of Education) of Nanchang Hangkong University, China. His main research interest has been the development of high-sensitivity laser spectrometer for laboratory and field studies of atmospheric trace gases and aerosols.

Huailin Zang received the B.E. degree in photoelectric information engineering from Hefei Normal University of Electronic Information Engineering in 2016. Since 2016, he has been a Graduate Student with the School of Measuring and Optical Engineering, Nanchang Hangkong University. His research interests include optical fiber sensing and gas absorption spectrum.

Qiang Wu received the B.S. and Ph.D. degrees from Beijing Normal University and Beijing University of Posts and Telecommunications, Beijing, China, in 1996 and 2004, respectively.,From 2004 to 2006, he worked as a Senior Research Associate in City University of Hong Kong. From 2006 to 2008, he took up a research associate post in Heriot-Watt University, Edinburgh, U.K. From 2008 to 2014, he worked as a Stokes Lecturer at Photonics Research Centre, Dublin Institute of Technology, Ireland. He is currently an Associate Professor at Northumbria University, U.K. His research interests include photonics devices and fiber optic sensing.

Weidong Chen received his B.S. (1992) from Zhongshan University, M.S. (1998) and Ph.D. degree (1991) from the University of Science and Technologies of Lille in France. He is full professor of physics at the University of the Littoral Opal Coast, Dunkerque, France. His current research interests include: development of photonic instrumentation for applied spectroscopy, optical metrology (concentration, isotope ratio) of trace gases for applications in atmospheric photochemistry and environmental science, and optical parametric laser source generation by frequency conversion and its applications to applied spectroscopy.

Chenwen Ye is a lecturer at the School of Measuring and Optical Engineering, Nanchang Hangkong University.

Xingdao He was born in Jingan, China, in 1963. He received the Ph.D. degree in optics from Beijing Normal University, Beijing, China, in 2005. He is currently a Professor with the Key Laboratory of Nondestructive Test (Ministry of Education), Nanchang Hangkong University, China. His current research interests include light scattering spectroscopy, optical holography, and information processing.